Classifying the Combined Influence of Shear Rate, Temperature, and Pressure on Crystalline Morphology and Specific Volume of Isotactic (Poly)propylene

Maurice H. E. Van der Beek,[†,‡] Gerrit W. M. Peters,[*,§] and Han E. H. Meijer[§]

TNO Science and Industry, Department of Design and Manufacturing, P.O. Box 6325, 5600 HE Eindhoven, The Netherlands, and Materials Technology, Dutch Polymer Institute, Eindhoven University of Technology, P.O. Box 513, 5600 MB Eindhoven, The Netherlands

Received April 5, 2006; Revised Manuscript Received November 1, 2006

ABSTRACT: The use of the Deborah number in classifying the effect of shear flow on the evolution of the specific volume and resulting crystalline morphology is investigated. We distinguish between flows applied at large undercoolings and flows applied at low undercoolings. In the first case, the Deborah number provides a good classification tool to determine the influence of flow on the evolution of orientation and structural properties of the crystalline morphology and specific volume. Both the Deborah number related to the process of chain retraction (De_s) or the Deborah number related to reptation of chains (De_{rep}) can equally well be used to classify the influence of flow on the evolution of specific volume, as characterized by the dimensionless transition temperature and dimensionless rate of transition. If, however, flow is applied at relatively low undercoolings, remelting of flow-induced crystalline structures and relaxation of molecular orientation play a significant role after cessation of flow. Therefore, in these cases the use of Deborah (or alternatively Weissenberg) numbers is found to be of little use in this classification. Note that the Deborah numbers are used as a classification parameter to distinguish between different crystallization regimes and not as the driving force for flow induced crystallization.

1. Introduction

For semicrystalline polymers, it is known that flow experienced during processing can strongly influence the resulting crystalline morphology[1−11] and as a consequence also the evolution of specific volume.[12−14] Not only the flow applied but also the pressure and temperature during flow, as well as the material's molecular weight distribution (MWD), influence the evolution of specific volume with temperature,[15] and it is the combination of these process conditions and material parameters that is indicative for the dynamics of crystallization. This makes predictions regarding the evolution of crystal structure and specific volume as influenced by flow rather complicated. Dimensionless Deborah (*De*) and Weissenberg (*We*) numbers proved to be useful in quantifying the strength of the flows applied at various processing conditions[16,17] and in classifying flow conditions with respect to their influence on the resulting crystalline morphology.[18] These numbers are respectively defined as

$$De = \frac{\tau}{t} \tag{1}$$

$$We = \dot{\gamma}\tau \tag{2}$$

where τ is a characteristic rheological relaxation time of the material, t a characteristic time of the process, and $\dot{\gamma}$ is the shear rate. Both numbers are identical when the characteristic time of the process t is chosen equal to the reciprocal value of the shear rate $\dot{\gamma}$. Acierno et al.[16] used *We* to study the influence of shear flow on crystallization of various grades of isotactic poly-(1-butene) (iPB), differing in molecular weight distribution (MWD), using a rotational rheometer equipped with plate−plate geometry. The Weissenberg number *We* was determined by setting τ equal to the maximum relaxation time resulting from small angle oscillatory shear (SAOS) rheological characterization tests. During isothermal crystallization experiments at 103 °C, the time needed to start crystallization and the (dimensionless) half-time for crystallization decreased with increasing *We*. Furthermore, a transition from spherulitic to "rod-like" crystallite growth was observed for roughly $We > 150$. Elmoumni et al.[17] performed isothermal flow-induced crystallization experiments on various grades of isotactic polypropylene (iPP) at a temperature of 145 °C. They also used a rotational rheometer, but with cone−plate geometry, to measure the rheology and they based *We* on the relaxation time associated with the crossover of G' and G''. In complete agreement with Acierno et al. they found the induction time for crystallization to decrease, and the rate of crystallization to increase, with increasing *We*. Additionally the orientation of the *c*-axis in the direction of flow, and the nucleation density, increased with increasing *We*. For $We < 1$ the resulting morphology showed a spherulitic structure, while for $We > 1$ shish kebab formation was observed. However, they noted that if *We* was defined based on the longest relaxation time, this critical value could shift with as much as 1 order of magnitude ($We > 10$). To over come the problem of *We* definition, Van Meerveld et al.[18] proposed a classification of flow-induced crystallization (FIC) including the effects on resulting crystalline morphology, based on values of the Deborah numbers *De*, associated with the process of reptation (De_{rep}) and chain retraction (De_s) of the molecules in the high molecular weight (HMW) tail; i.e., De_{rep} and De_s should correspond to the relaxation dynamics of the HMW tail. De_{rep} can be regarded as a measure for the ability of the flow to orient the contour path of molecules while De_s is a measure for the ability of the flow to stretch the contour path of molecules. From their analysis of FIC experiments using iPP reported in literature, they found that the effect of flow on the number density of nuclei already

* Corresponding author. E-mail: g.w.m.peters@tue.nl.
† TNO Science and Industry, Department of Design and Manufacturing.
‡ At present this author is working at Philips Applied Technologies. E-mail: maurice.van.der.beek@philips.com.
§ Materials Technology, Dutch Polymer Institute, Eindhoven University of Technology.

10.1021/ma060768p CCC: $33.50
Published on Web 12/07/2006

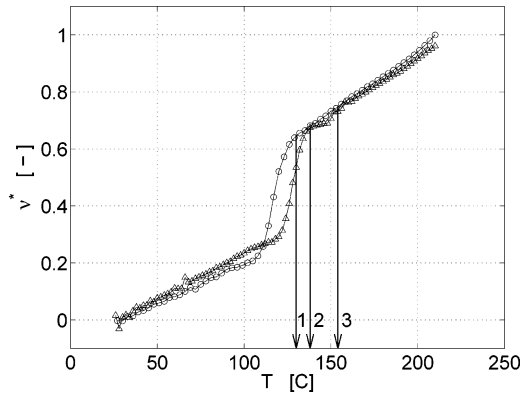

Figure 1. Example of the normalized specific volume ν^* measured during quiescent conditions (○) and when applying shear flow at a temperature of 154 °C (Δ): (1) transition temperature, T_{tQ}; (2) transition temperature, $T_{t\gamma}$; (3) temperature where shear flow is applied, T_γ.

starts at $De_{rep} > 1$, $De_s < 1$ while for $De_{rep} > 1$, $De_s = 1-10$, a transition from spherulitic to shish kebab formation was observed.

All these studies used the Weissenberg and Deborah numbers to analyze, and classify, the influence of flow on the resulting crystalline morphology, when flow is applied during isothermal conditions and atmospheric pressure. Furthermore, classification of the influence of flow on the morphology of iPP[17,18] was typically limited to experiments performed at a fairly large undercooling $\Delta T = 36 - 46$ °C (assuming an equilibrium melting temperature T_m^0 at atmospheric pressure of 186 °C).[19] Now the question arises whether the Deborah and Weissenberg numbers can similarly be used to classify the influence of flow on the crystalline morphology when flow is applied during conditions relevant for industrial processing of polymers, i.e., elevated pressures and non-isothermal conditions. A second question is whether these dimensionless numbers can be used to classify the influence of flow applied on the evolution of specific volume? In this study we try to answer both questions and we analyze the use of the Deborah number for classifying the influence of shear flow on the resulting crystalline morphology and evolution of specific volume applying flows at elevated pressures, at various degrees of undercooling, and under non-isothermal conditions.

2. Methods

2.1. Deborah Numbers. To quantify the strength of the shear flow applied at various elevated pressures and temperatures, we define the Deborah number as

$$De = a_T a_P \tau \dot{\gamma} \tag{3}$$

where τ is a characteristic rheological relaxation time of the material at a reference temperature T_{ref} and reference pressure P_{ref}, $\dot{\gamma}$ is the shear rate applied, a_T is the temperature shift factor, and a_P the pressure shift factor. Temperature shifting is done according to a WLF-description:

$$log(a_T) = -\frac{c_1(T - T_{ref})}{c_2 + (T - T_{ref})} \tag{4}$$

with T the absolute temperature, T_{ref} a reference temperature, and WLF constants $c_1 = 2.018$ and $c_2 = 2.686 \times 10^2$.[11]

The pressure shift a_P is defined according to[20]

$$a_P = \exp\left(\frac{\kappa P}{T}\right) \tag{5}$$

where $\kappa = 8.405 \times 10^{-6}$ K/Pa, and it assumed a generic value for polypropylene, P the pressure, and T the absolute temperature. The shear flow experiments performed in this study are, subsequently, classified according to the method proposed by Van Meerveld et al.,[18] because Deborah numbers De_{rep} and De_s are closely correlated to the dynamics of the chains in the HMW tail, which are known to greatly influence the crystallization process under flow.[3,8,10] The definitions are

$$De_{rep} = \frac{\tau_{rep}}{t} \tag{6}$$

$$De_s = \frac{\tau_s}{t} \tag{7}$$

The relaxation times τ_{rep} and τ_s of the longest chains of the MWD are estimated according to[21,22]

$$\tau_{rep} = 3\tau_e Z^3\left(1 - \frac{1.51}{\sqrt{Z}}\right)^2 \tag{8}$$

$$\tau_s = \tau_e Z^2 \tag{9}$$

with τ_e being the equilibrium time, which is independent of the molecular weight of the chain,[21,23,24] and Z representing the number of entanglements per chain:

$$Z = M_{HMW}/M_e \tag{10}$$

Here M_{HMW} is the largest molecular weight of the MWD measured via gel permeation chromatography (GPC), and M_e is the molar mass between entanglements.

2.2. Dimensionless Transition Temperature. The transition temperature T_t is a characteristic feature of the evolution of specific volume that is significantly influenced by the combination of shear rate, temperature and pressure during flow.[15] To be able to compare the influence of flow applied at various processing conditions on the transition temperature, we introduce the dimensionless transition temperature θ_t defined as

$$\theta_t = \frac{T_t\gamma - T_\gamma}{T_{t_Q} - T_\gamma} \tag{11}$$

where $T_{t\gamma}$ is the transition temperature in case shear flow is applied, T_γ the temperature during shear flow, and T_{tQ} the transition temperature in case no shear flow is applied, i.e., resulting from quiescent crystallization (see also Figure 1).

2.3. Dimensionless Transition Rate. In analogy to the dimensionless transition temperature θ_t, we introduce a dimensionless rate of transition λ defined as

$$\lambda = \left(\frac{\partial \nu}{\partial T}\right)_\gamma / \left(\frac{\partial \nu}{\partial T}\right)_Q \tag{12}$$

where $(\partial\nu/\partial T)$ is the average transition rate of the specific volume with temperature. The suffix γ indicates the transition rate obtained when shear flow is applied, and the suffix Q indicates the rate of transition resulting from quiescent conditions. Note that both θ_t and λ refer to a relative change in T_t and the rate of transition with respect to quiescent conditions, the latter being dependent on cooling rate and pressure.

3. Experimental

3.1. Materials. Two commercial grades isotactic polypropylenes (iPP) with various molecular weights ($\bar{M}_w$) were used. The first (iPP-1) is supplied by Borealis (grade HD120MO), and is characterized by $\bar{M}_w = 365000$ g/mol, $\bar{M}_w/\bar{M}_n = 5.2$. The second (iPP-2) is supplied by DSM (grade Stamylan P 13E10) and is characterized by $\bar{M}_w = 636000$ g/mol, $\bar{M}_w/\bar{M}_n = 6.9$. Figure 2 shows the molecular weight distribution of both materials determined via GPC. Notice that the iPP-2 was also

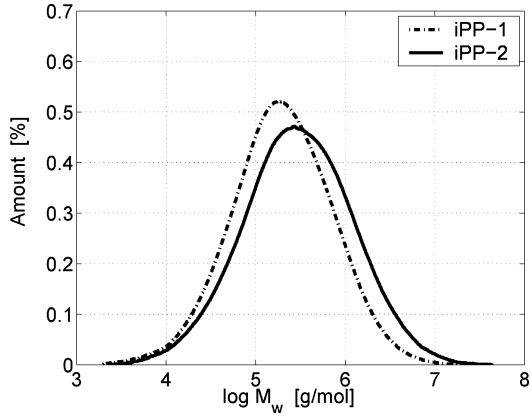

Figure 2. Molecular weight distribution determined via gel permeation chromatography (GPC). Data were provided by Gahleitner/Königsdorfer (Borealis, Linz, Austria).

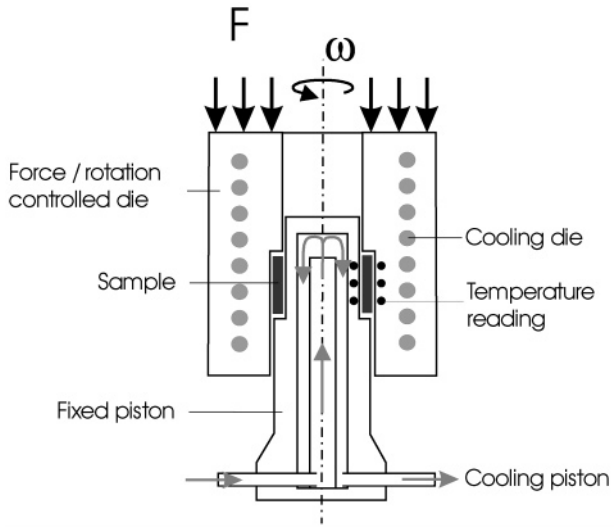

Figure 3. Working principle of the custom designed dilatometer.

Table 1. Equilibrium Time τ_e, Relaxation Time τ_{rep} Associated to the Process of Reptation, and Relaxation Time τ_s Associated to the Process of Retraction of Chains in the HMW-tail, at a Reference Temperature of 190 °C and Reference Pressure of 1.0 × 10^5 Pa.

material	M_{HMW} [10^7 g/mol]	Z	τ_e [10^{-8} s]	τ_{rep} [10^4 s]	τ_s [s]
iPP-1	2.40	5469	3.54	1.7	1.0
iPP-2	4.37	9891	3.54	10.0	3.5

used by Swartjes et al.,[11] but our results of GPC characterization are somewhat different. Samples with dimensions 2.5 × 65 × 0.4 mm were prepared by compression molding, for 3 min at 210 °C with a force of 50 kN, and subsequently cooled in a water cooled press during 5 min from 210 to 25 °C, again with a force of 50 kN.

In accordance with Van Meerveld et al.,[18] for both iPP's, an equilibrium time $\tau_e = 3.54 \times 10^{-8}$ s is taken. This value of τ_e is found by a procedure that uses the zero shear viscosity η_0 and the molar mass between entanglements, $M_e = 4400$ g/mol[25] and a reference temperature of 190 °C. Time−temperature shifting is performed using the temperature shift factor a_T. Table 1 lists the values for relaxation times τ_{rep} and τ_s calculated using eqs 8 and 10. Deborah numbers De_{rep}, De_s are determined using eqs 6 and 7.

3.2. Experimental Techniques. The influence of shear flow on specific volume at elevated pressures is investigated using a custom designed dilatometer as schematically shown in Figure 3. The dilatometer has an annular shaped sample spacing with

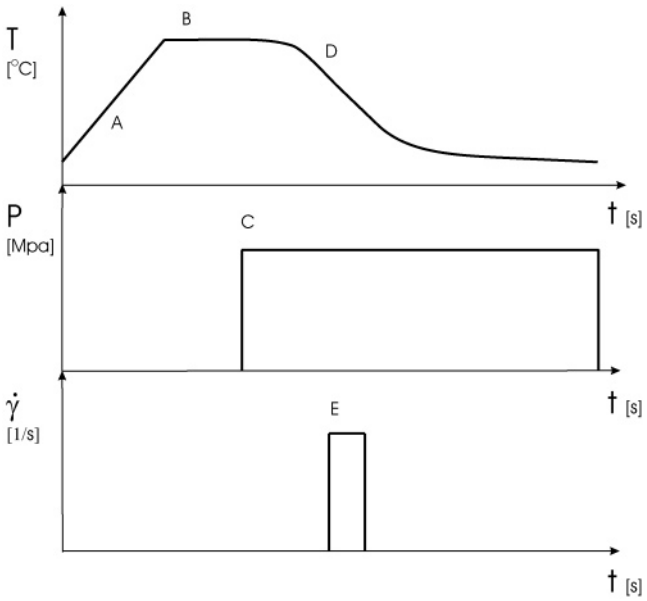

Figure 4. Schematic representation of the employed experimental procedure: (A) heating, (B) thermal equilibration, (C) pressurizing, (D) start of cooling, and (E) applying shear flow.

an inner radius $r_i = 10.50$ mm and outer radius $r_o = 11.00$ mm. Cooling of the sample is performed simultaneously from its inside and outside; i.e., from each side a sample thickness of 0.25 mm is cooled by conduction. The height of the sample can be arbitrarily chosen to a maximum of 10 mm but is here set to 2.0−2.5 mm. Because of this axi-symmetric design, the sample can be sheared by rotating the outer part of the device, similar to a Couette rheometer. A more detailed description of the dilatometer is given in Van der Beek et al.[26] where also a comparison was made with specific volume data measured using a conventional "bellows" type dilatometer, showing relative differences in measured specific volume of 0.1−0.4%.

Dilatometer experiments are performed in the isobaric cooling mode according to the procedure schematically depicted in Figure 4: (A) the sample is heated with an average heating rate of 5 °C/min to a temperature of 210 °C; (B) the sample is kept for 10 min at 210 °C to ensure full melting of the crystalline microstructure, (C) pressurized to the desired level, and (D) cooled to room temperature during which the pressure is maintained constant to within ±0.3 MPa, (E) and during cooling subjected to shear flow for a certain time and constant shear rate. After the sample is completely cooled down, it is taken out of the dilatometer and the same procedure is repeated in the absence of a sample. This calibration measurement is used to correct the measured volumetric change of the sample for external influences such as thermal expansion of the dilatometer, deformation of the dilatometer due to mechanical loading, etc. Note that shear flow is applied over a range in the temperatures given the non-isothermal conditions. Therefore, T_γ refers to the average temperature during flow and the thermal shift factor a_T is determined using T_γ.

The final crystalline structure is evaluated using wide-angle X-ray diffraction (WAXD) and scanning electron microscopy (ESEM). WAXD experiments were performed ex-situ at the materials beamline ID 11 of the European Synchrotron Radiation Facility (ESRF) in Grenoble, France. Actual experiments were performed on a representative piece of the ringlike samples that resulted from dilatometer experiments (Figure 5). The size of the X-ray beam is 0.2 × 0.2 mm^2, having a wavelength of 0.4956 Å. The beam passes through the sample in a direction parallel to the initial direction of cooling and perpendicular to

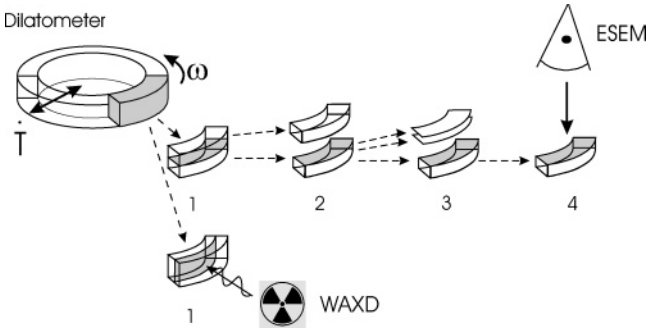

Figure 5. Schematic representation of the sample preparation procedure performed on a representative piece cut from the ringlike samples as obtained from dilatometer experiments (1). For WAXD experiments, no additional sample preparation is performed. For ESEM experiments, this piece is further cut across its approximate center line and parallel to the direction of flow (2). Coupes are taken under cryogenic conditions in order to smoothen the surface (3). The final sample piece is subjected to an acidic solution and the surface is treated with a gold (Au) layer for visualization by ESEM (4).

the direction of applied flow. Because the curvature of the sample is much larger than the dimensions of the beam, the effect of this curvature on the diffraction pattern is assumed negligible. The detector used is a Frelon CCD detector with 1024 × 1024 pixels. Both horizontal and vertical pixels are 164 μm in size. From calibration experiments, using lanthanum hexaboride, a sample-to-detector distance of 439.9 mm was determined. The exposure time for all images was 30 s. Additionally, ESEM experiments are performed to visualize the crystalline morphology of samples. Again, a representative piece is taken from the ringlike samples resulting from dilatometer experiments. Samples are cut across their approximate center line and parallel to the direction of applied flow (Figure 5). The surface of one of the sample halves is smoothed by taking microtome cuts under cryogenic conditions. The final sample is subsequently etched for 4 h in a mixture of potassium permanganate ($KMnO_4$) and acid (4 vol % H_3PO_4, 10 vol % H_2SO_4) and coated with gold (Au). Finally, imaging of the etched sample surface was done with a Philips XL30 ESEM using a SE-detector and operated at 5 kV.

Table 2. Overview of Deborah Numbers De_{rep}, De_s Resulting from Shear Flow Applied at Temperatures T_γ, at a Pressure of 40 MPa and a Shear Rate of 39 1/s.

material	T_γ [°C]	$De_{rep} \times 10^6$	$De_s \times 10^2$
iPP-1	138.6	6.4	4.1
iPP-1	154.1	3.7	2.4
iPP-1	193.0	1.3	0.8
iPP-2	133.0	39.2	13.6
iPP-2	152.5	24.2	8.4
iPP-2	192.5	7.5	2.6

4. Results and Discussion

4.1. Classification of the Resulting Crystalline Morphology. We subjected samples of both materials to a shear rate of

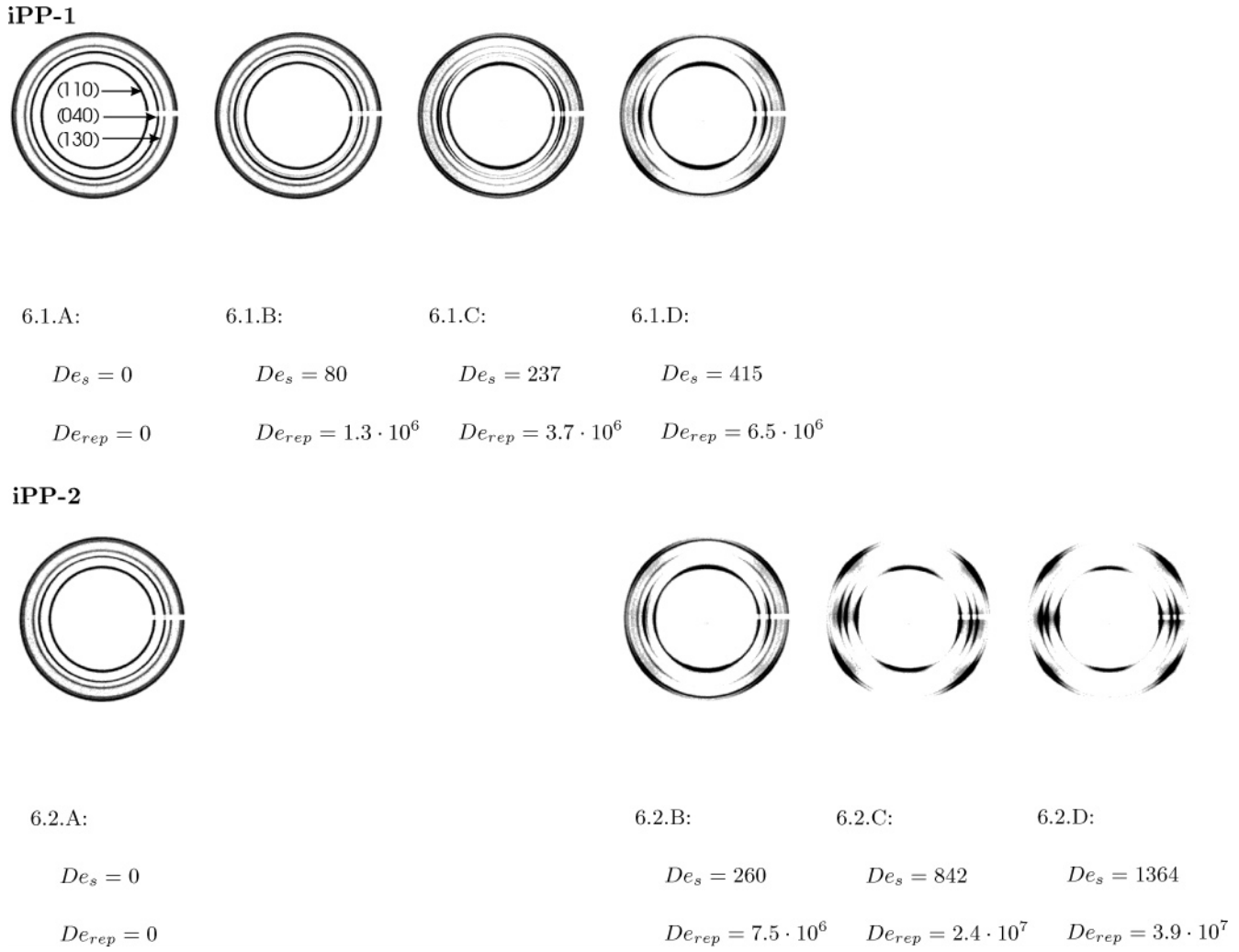

Figure 6. Orientation of the crystalline morphology of samples subjected to a shear rate of 39 1/s, a pressure of 40 MPa, and a cooling rate of 1.4 °C. Variation in Deborah numbers De_s, De_{rep} is the result of shearing at different temperatures, see also Table 2.

Table 3. Summary of the Morphology Features Observed in Figure 7 as a Function of Deborah Numbers De_{rep}, De_s, Where S = Spherulitic, R = Row Nucleated, and K = Shish Kebab.

material	figure	ΔT_γ [°C]	$De_s \times 10^2$	$De_{rep} \times 10^6$	morphology
iPP-1	7.1.B	2.0	0.8	1.3	S
iPP-1	7.1.C	40.9	2.4	3.7	R, S
iPP-2	7.2.B	2.5	2.6	7.5	R, S
iPP-1	7.1.D	56.4	4.1	6.4	K, R, S
iPP-2	7.2.C	42.5	8.4	24.2	K, R
iPP-2	7.2.D	62.0	13.6	39.2	K

39 1/s for a shear time of 3 s, a pressure of 40 MPa, and an average cooling rate during crystallization of 1.4−2.0 °C/s. It was shown in an earlier study[27] that the use of these cooling rates results in homogeneous cooling of the sample; i.e., in quiescent crystallization experiments a uniform distribution of the degree of crystallinity across the thickness of the sample was derived from wide-angle X-ray diffraction (WAXD) measurements. A variation in Deborah number is achieved by applying the shear flow at different temperatures; see Table 2. Note that the values for De_s and De_{rep} are of the same order of magnitude as found by Van Meerveld et al.,[18] where he is also using the HMW tail to define the Deborah numbers. Figure 6 shows the orientation of crystals as visualized by WAXD analysis. The main reflections of the crystallographic planes (110), (040), and (130) of the α-crystalline phase are indicated for reference. The direction of flow in all pictures is vertical.

Figures 6.1.A and 6.2.A show WAXD images of samples crystallized in quiescent conditions, i.e., $De_s = 0$, $De_{rep} = 0$. Generally, an increase in the orientation of crystals is observed with higher De_s and De_{rep}. When subjecting iPP-1 to a flow characterized by $De_s = 80$ and $De_{rep} = 1.3 \times 10^6$ the influence of flow on the resulting orientation of crystals is negligible (Figure 6.1.B). However, the presence of the $(300)_\beta$ reflection, located between the $(110)_\alpha$ and $(040)_\alpha$ reflections, is evidence of the flow applied. Compared to results of Van Meerveld et al., who observed shish-formation for $De_{rep} > 1$ and $De_s = 1-10$, the flow applied can be regarded as very strong. We now define $\Delta T_\gamma = T_m^0 - T_\gamma$ to be the undercooling specifically referring to temperature T_γ where shear flow is applied. For $T_\gamma = 193$ °C an undercooling in the range of $\Delta T_\gamma = 2 - 5$ °C can be assumed, considering an equilibrium melting temperature of about $T_m^0 = 195$ °C (for the α-phase) to $T_m^0 = 198$ °C (for the γ-phase) at a pressure of 40 MPa.[19] Given this fairly low undercooling at which the flow is applied, remelting of flow induced crystalline structures and relaxation of molecules after cessation of flow are thought to play a significant role, such that the influence of flow on the orientation of the crystalline morphology is completely erased. By comparison, flow applied on iPP-2 at approximately the same undercooling (Figure 6.2.B) does have a significant effect on the orientation of crystals. This is explained by the higher $\bar{M}_w$ and associated larger relaxation times of iPP-2, resulting in a stronger flow and slower relaxation of molecular orientation after cessation of flow. The increased strength of flow not only results in a higher orientation of chains but also results in a higher number of chains oriented,[6] potentially leading to a higher number of flow-induced nuclei.

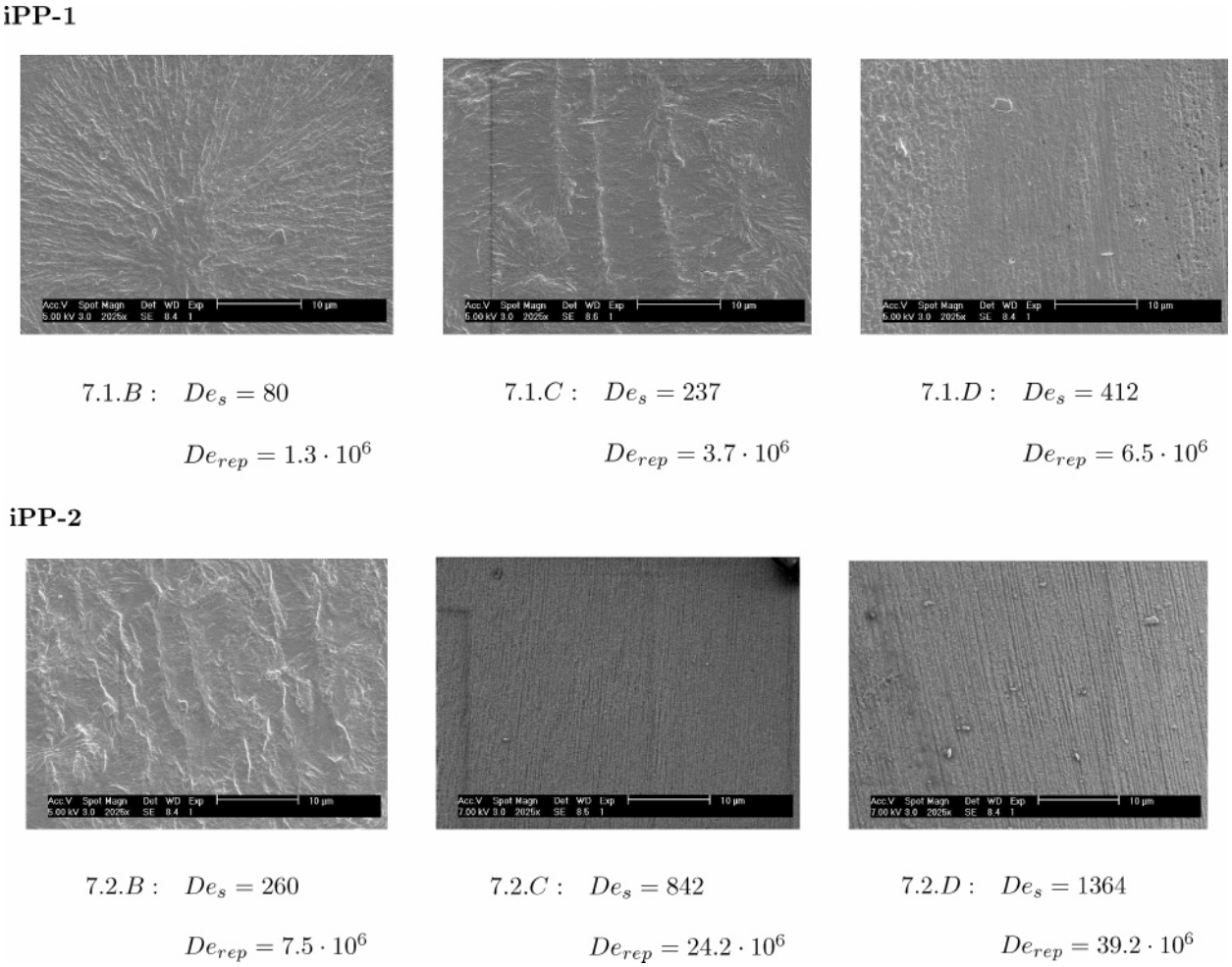

Figure 7. Crystalline morphology visualized by ESEM of samples subjected to a shear rate of 39 1/s, a pressure of 40 MPa, and a cooling rate of 1.4 °C. Variation in Deborah numbers De_s, De_{rep} is the result of shearing at different temperatures, see also Table 2.

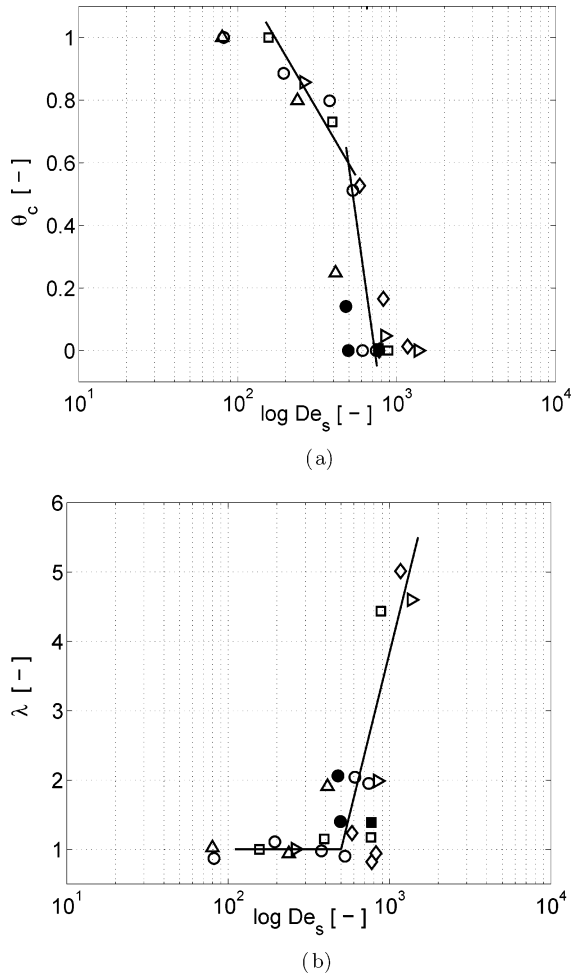

Figure 8. Dimensionless transition temperature θ_t and the dimensionless rate of transition λ as a function of Deborah number De_s: (●) iPP-1a; (■) iPP-1b; (○) iPP-1c; (□) iPP-1d; (◇) iPP-1e; (Δ) iPP-1f; (triangle pointing right) iPP-2.

Note: since analysis of the crystalline fractions in all samples subjected to the processing conditions in our study shows a prevailing α-fraction,[27] for the sake of argument $T_m^0 = 195$ is further used to quantify the undercooling at which samples are subjected to shear flow.

Comparing the Deborah numbers of Figure 6.2.B with those of Figure 6, parts 1.C and 1.D, a higher degree of orientation is expected but not found. This also points to the influence of remelting and molecular relaxation, (partially) erasing the effect of flow. Flow applied at undercooling ranging from $40.9 \leq \Delta T_\gamma \leq 62.0$ is depicted in Figure 6, parts 1.C, 2.C, 1.D, and 2.D (see also Table 3). The influence of remelting and relaxation is expected to be negligible at these undercoolings.[17] Consistent with an increase in De_s and De_{rep}, an increase in orientation is observed. Important features that can be related to orientation of chains in the direction of flow are the equatorial reflections of the $(110)_\alpha$ and $(040)_\alpha$ crystallographic planes. These can already be observed for $De_s = 237$ but are significantly present for $De_s \geq 842$. Visualizing the morphology using ESEM (see Figure 7) reveals more details about the structures formed. The numbering of subfigures corresponds to Figure 6. As already discussed, for iPP-1 the influence of shear flow applied at small undercooling is negligible (Figure 7.1.B). Large spherulites are visible of up to 50 μm in size across the sample. However, iPP-2 samples subjected to shear flow applied at identical conditions already show significant orientation of the morphology. The bright lines in Figure 7.2.B are thought to be short row nucleated structures, observed at the core of the sample. At the edges, a somewhat stronger row nucleated morphology is observed with row lengths exceeding 20 μm and width of about 500 nm. If shear flow is applied to iPP-1 at an undercooling $\Delta T_\gamma = 40.9$ °C, Figure 7.1.C, a mixture of spherulites and row nucleated structures is observed. Spherulites are typically about 10−20 μm in size while rows are about 30 μm in length and 500 nm wide. Again, compared to iPP-1, the morphology of iPP-2 is much more affected by the shear flow at $\Delta T_\gamma = 42.5$ °C. Figure 7.2.C clearly shows an abundant presence of densely packed and highly oriented crystallites "shish kebabs" . Finally, shearing iPP-1 at an even higher undercooling of $\Delta T_\gamma = 56.4$ °C, Figure 7.1.D, results in a mixed morphology of row nucleated and spherulitic crystallites in the core while additionally sporadic shish kebab formation is observed at the edge. The morphology of iPP-2 sheared at $\Delta T_\gamma = 62.0$ °C consists completely of shish kebabs, both at the core and edges of the sample. Typically, these shish kebabs are about 270 nm wide and have a periodicity of kebabs ranging from 200 to 450 nm. Table 3 summarizes the morphologies observed as a function of Deborah number. The presence of spherulitic (S), row-nucleated (R), and shish kebab (K) morphology shows a logical order with increasing Deborah number. Because of the expected remelting present in Figure 7, parts 1.B and 2.B, the transition from spherulitic to row-nucleated morphology is difficult to determine. The transition to shish kebab morphology occurs for $240 \leq De_s \leq 410$, and saturation of the morphology with shish kebab structures happens for $842 \leq De_s \leq 1364$.

Table 4. Overview of Processing Conditions Applied and Resulting Deborah Numbers De_{rep}, De_s

material	P [MPa]	$\dot{T}$ [°C/s]	$\dot{\gamma}$ [1/s]	T_γ [°C/s]	$De_{rep} \times 10^6$	$De_s \times 10^2$	remark
iPP-1	20	0.1	78	141.5	7.8	5.0	iPP-1a
				142.5	7.5	4.8	
	40	0.1	78	140.2	12.2	7.7	iPP-1b
	20	1.2	78	127.4	11.7	7.4	iPP-1c
				131.0	9.6	6.1	
				140.0	8.3	5.3	
				150.1	5.9	3.8	
				169.6	3.1	1.9	
				210.0	1.3	0.8	
	40	1.4	39	138.6	6.4	4.1	iPP-1d
				154.1	3.7	2.4	
				193.0	1.3	0.8	
	40	1.4	78	131.8	13.9	8.8	iPP-1e
				141.2	12.0	7.7	
				153.6	7.7	3.9	
				200.6	2.4	1.5	
	60	1.4	78	140.2	18.4	11.7	iPP-1f
				150.4	12.9	8.2	
				151.3	12.2	7.7	
				160.7	9.2	5.9	
iPP-2	40	1.4	39	133.0	39.2	13.6	iPP-2
				152.5	24.2	8.4	
				192.5	7.5	2.6	

4.2. Classification of the Evolution of Specific Volume. Figure 8 shows the dimensionless transition temperature θ_t and dimensionless rate of transition λ as a function of Deborah number De_s. Variation in Deborah number was achieved by variation of shear rate, temperature during flow T_γ, and pressure level (see also Table 4). Also the cooling rate was varied. However, probably because of the relatively large undercoolings at which the shear flow was applied, the variation in cooling rate did not show a significant influence. The use of De_{rep} gives qualitatively the same trend of θ_t and λ, since for the values of Z of the materials used the ratio of De_{rep} and De_s is approximately constant and equal to 3 times Z. Lines are drawn to guide the eye. If De_s is lower than a minimum value of

approximately $De_s = 150$, the influence of flow on the evolution of specific volume is negligible ($\theta_c = 1$, $\lambda = 1$). Typically, in our experiments this corresponds to shear flow applied to iPP-1 at small undercooling (Figures 6.1.B and 7.1.B). When this value is superseded, at first only a shift of the transition temperature toward higher values is observed ($0.6 \leq \theta_c \leq 1$), while the average rate of transition is unaffected ($\lambda = 1$). In our experiments, this corresponds to flow applied to iPP-1 at large undercooling (Figures 6.1.C and 7.1.C) and flow applied to iPP-2 applied at small undercooling (Figures 6.2.B and 7.2.B). With increasing De_s, the influence of flow on the shift of the transition temperature shows a strong increase ($0.6 < \theta_c \leq 0$). Additionally, the rate of transition increases with maximum a factor 2. Interestingly, the upswing of λ at about $De_s = 500$ correlates rather well with the transition from spherulitic to shish kebab morphology ($240 \leq De_s \leq 410$). Finally, for approximately $De_s \geq 800$, the crystallization process is enhanced such that the transition from the melt to the semicrystalline state starts almost instantaneously the moment flow is applied ($\theta_c = 0$). Therefore, a significant part of the flow is applied during crystallization. This is associated with a significant increase in the rate of transition ($4.5 \leq \lambda \leq 5$). Note that the classification of flow applied at large undercooling is hardly affected by differences in cooling rate.

5. Conclusions

Classification of the influence of flow on the resulting crystalline morphology was performed for two isotactic polypropylene grades, differing in molecular weight distribution, subjected to flow at constant elevated pressure and during nonisothermal conditions. Variation in the strength of the flow applied was reached by shearing at different degrees of undercooling. Classification of the influence of flow on the orientation of the resulting crystalline morphology as visualized by WAXD could be performed if flow was applied at relatively large undercoolings. Applied flow at high temperatures and relatively low undercoolings leads to a substantial influence of remelting and relaxation of molecular orientation obscuring the effect of the Deborah number. These conclusions also hold for the classification of the influence of flow on the evolution of specific volume. If flow is applied at large undercooling, De_s and De_{rep} can equally well be used to classify the influence of flow on the dimensionless transition temperature and dimensionless transition rate. Even relatively large differences in cooling rate have little effect on these results of the successful classification. Finally, one should be aware that the Deborah numbers are used as a classification parameter to distinguish between different crystallization regimes and not as the driving force for flow induced crystallization.

References and Notes

(1) Jerschow, P.; Janeschitz-Kriegl, H. *Rheol. Acta* **1996**, *35*, 127−133.

(2) Tribout, C.; Monasse, B.; Haudin, J. M. *Colloid Polym. Sci.* **1996**, *274*, 197−208.

(3) Vleeshouwers, S.; Meijer, H. E. H. *Rheol. Acta* **1996**, *35*, 391−399.

(4) Keller, A.; Kolnaar, J. W. H. In *Processing of Polymers*; Meijer, H. E. H., Ed.; VCH: New York, 1997; Vol. 18, pp 189−268.

(5) Eder, G.; Janeschitz-Kriegl, H. In *Processing of Polymers*; Meijer, H. E. H., Ed.; VCH: New York, 1997; Vol. 18, pp 269−342.

(6) Somani, R. H.; Hsiao, B. S.; Nogales, A. *Macromolecules* **2000**, *33*, 9385−9394.

(7) Kumaraswamy, G.; Kornfield, J. A.; Yeh, F.; Hsiao, B. S. *Macromolecules* **2002**, *35*, 1762−1769.

(8) Seki, M.; Thurman, D. W.; Oberhauser, J. P.; Kornfield, J. A. *Macromolecules* **2002**, *35*, 2583−2594.

(9) Koscher, E.; Fulchiron, R. *Polymer* **2002**, *43*, 6931−6942.

(10) Janeschitz-Kriegl, H.; Ratajski, E.; Stadlbauer, M. *Rheol. Acta* **2003**, *42*, 355−364.

(11) Swartjes, F. H. M.; Peters, G. W. M.; Rastogi, S.; Meijer, H. E. H. *Int. Polym. Proc.* **2003**, *18*, 53−66.

(12) Fritzsche, A. K.; Price, F. P. *Polym. Eng. Sci.* **1974**, *14*, 401−412.

(13) Fleischmann, E.; Koppelmann, J. *J. Appl. Polym. Sci.* **1990**, *41*, 1115−1121.

(14) Watanabe, K.; Suzuki, T.; Masubuchi, Y.; Taniguchi, T.; Takimoto, J.; Koyama, K. *Polymer* **2003**, *44*, 5843−5849.

(15) Van der Beek, M. H. E.; Peters, G. W. M.; Meijer, H. E. H. Influence of shear flow on the specific volume andcrystalline morphology of isotactic polypropylene. *Macromolecules* **2006**, *34*, 1805−1814.

(16) Acierno, S.; Palomba, B.; Winter, H. H.; Grizutti, N. Effect of molecular weight on the flow-inducedcrystallization of isotactic Poly-(1-butene). *Rheol. Acta* **2003**, *42*, 243−250.

(17) Elmoumni, A.; Winter, H. H.; Waddon, A. J. Correlation of material and processing time scales withstructure development in isotactic polypropylene crystallization. *Macromolecules* **2003**, *36*, 6453−6461.

(18) Van Meerveld, J.; Peters, G. W. M.; Hütter, M. Towards a rheological classification of flow inducedcrystallization experiments of polymer melts. *Rheol. Acta* **2004**, *44*, 119−134.

(19) Mezghani, K.; Phillips, P. The gamma-phase of high molecular weight isotacticpolypropylene: III. the equilibrium melting point and the phasediagram. *Polymer* **1998**, *39*, 3735−3744.

(20) Kadijk, S. E.; Van Den Brule, B. H. A. A. On the Pressure Dependency of the Viscosity of Molten Polymers. *Polym. Eng. Sci.* **1994**, *34*, 1535−1546.

(21) Doi, M.; Edwards, S. F. *The theory of polymerdynamics*; Claredon Press: Oxford, U.K., 1986.

(22) Ketzmerick, R.; Öttinger, H. C. Simulation of a non-markovian process modeling contour lengthfluctuation in the Doi-Edwards model. *Continuum Mech. Thermodyn.* **1989**, *1*, 113−124.

(23) Watanabe, H. Viscoelasticity and dynamicsof entangled polymers. *Prog. Polym. Sci.* **1999**, *24*, 1253−1403.

(24) Tube theory of entangled polymer dynamics. *Adv. Phys.* **2002**, *51*, 1379−1527.

(25) Van Meerveld, J. A method to extract the monomer frictioncoefficient from the linear viscoelastic behavior of linear, entangled polymer melts. *Rheol. Acta* **2004**, *43*, 615−623.

(26) Van der Beek, M. H. E.; Peters, G. W. M.; Meijer, H. E. H. A dilatometer to measure the influence of coolingrate and melt shearing on specific volume. *Int. Polym. Proc.* **2005**, *20*, 111−120.

(27) Van der Beek, M. H. E.; Peters, G. W. M.; Meijer, H. E. H. The influence of cooling rate on the specific volumeof isotactic poly-(propylene) at elevated pressures. *Macromol. Mater. Eng.* **2005**, *290*, 443−455.

MA060768P